SLIP IMPACT ON FLUID FLOW AND HEAT TRANSPORT IN THE BOUNDARY LAYER OVER A FLAT PERMEABLE PLATE-A COMPARATIVE STUDY

Abstract

An investigation is undertaken to compare and examine the influence of partial slip on the flow and heat transport of Newtonian and viscoelastic fluids within the boundary layer overa flat permeable plate. Navier-Stokes equation of motion is considered for Newtonian viscous incompressible fluid while the Walters Liquid (Model B′) is taken for viscoelastic non-Newtonian fluid. Special forms of slip factors for velocity and temperature involving local Reynolds number are considered. By employing similarity variables, the fluid flow guided equations, along with the corresponding boundary conditions, are reduced to self-similar form. Subsequently, these equations are evaluated using the 'bvp4c' solver, which is built-in within MATLAB. The results obtained from numerical computations are graphically represented for both Newtonian and viscoelastic fluids, considering different values of flow feature factors. The impact of slip and other flow dominating parameters on the flow and heat transport of both Newtonian and viscoelastic fluids are analysed from a physical perspective.

Keywords: Boundary layer, Heat transfer, Partial slip, Skin friction, Viscoelastic fluid

Author

Kamal Debnath
Associate Professor &HOD
Department of Mathematics
The Assam Royal Global University
Guwahati-35, Assam, India.
kamal.debnath@rgi.edu.in

I. INTRODUCTION

Recently, there has been significant interest in studying the heat transportphenomena of Newtonian boundary layer fluids flowing past a permeable plate embedded in porous medium. This attention is driven by the various applications in different engineering fields, including enhanced petroleum resource recovery and catalytic reactors. The viscoelastic fluid has little temperature and salinity sensitivity and is easily regulated by rheology. The viscoelastic fluid technology generates highly efficient fractures with low damage to conductivity, providing excellent control of fluid loss and high properties of proppant transport to generate the geometry of design fractures. The rheology of such a fluid is used to enhance biomodelling. Biofilms are also viscoelastic materials that are capable of dissipating energy from external forces and overcoming external mechanical stresses.The viscoelastic boundary layer fluid motion through permeable surfaces along withheat transport in the presence of partial slip has influenced researchers a lot these days. Such a flow has lots of applications in filtration and purification processes, metal processing, heat exchangers, catalytic reactors, insulation, etc. The physical concept of temperature variation between the plate and the surrounding fluid has many geothermal and engineering applications.

The velocity growth within the boundary layer during fluid motion across a flat surface was first studied by Blasius [1]. Pohlhausen [2] examined the heat transport phenomenon based on Blasius's findings, while Howarth [3] conducted a subsequent investigation into the numerical results obtained by Blasius. Cheng and Minkowycz [4] introduced a study on the fluid flow occurring in a porous media as a result of natural convection.With the use of numerical analysis, Mukhopadhyay and Layek [6] determined the mechanism of convective heat transfer in a boundary layer flow across a permeable plate. They also examined the influence of radiation on the temperature distribution.

Ishak [7] examined the flow behaviour and heat transportmechanism across a permeable plate while taking into account convective heating at the boundary surface. Bhattacharyya et al. [8] used the shooting method to undertake a numerical study of the flow of fluid in the boundary layer across a flat, moving surface. Bhattacharyya and Layek [9] also presented the solute diffusion due to the chemical reaction for boundary layer Newtonian fluid past a permeable plate. Abbas et al. [10] studied the heat transfer phenomenon taking slip condition at the boundary of viscous fluid past an infinite oscillating sheet. Khan et al. [11] demonstrated the heat transport and slip effects over a flat surface for carbon nanotubes. Ambreen et al. [12] discussed the heat transport and slip impact on hydromagnetic peristaltic non-Newtonian fluid flow. Sarojamma et al.[13] studied the stratified casson fluid motion and the heat transition, taking radiation effects into account.

The literature survey reveals that very few work has been carried out for comparative study of Newtonian fluid and viscoelastic fluidsover a flat permeable plate considering partial slip condition. Thus, the purpose of this work is to contrast the behaviour of Newtonian and viscoelastic fluids in the boundary layer over a porous flat plate as a result of partial slip. Navier-Stokes equation of motion is considered for Newtonian fluid, while Walters Liquid (Model $B^{'}$) [14, 15] is employed for viscoelastic fluid. The 'bvp4c' solver in MATLAB is used to solve the self-similar reduced fluid guided equations and their associated boundary conditions.The numerical results obtained were then presented graphically to analyse the influence of various flow feature parameters for further discussion.

1. **Mathematical Formulation:** The steady fluid motion in the boundary layer for both Newtonian and viscoelastic fluids flowing over a flat porous plate, taking into account the presence of slip effects, is investigated. The fluid model depicting the geometry of flow is shown in Figure 1.

   The fluid flowis described by the following set of equations:

$$u_x + v_y = 0 \quad (2.1)$$

$$uu_x + vu_y = \nu u_{yy} - \mathrm{k}_0(\rho)^{-1}\left(uu_{xyy} + vu_{yyy} - u_y u_{xy} - v_y u_{yy}\right) - \nu(\mathrm{k})^{-1}(u - U_\infty) \quad (2.2)$$

$$uT_x + vT_y = K\left(\rho C_p\right)^{-1} T_{yy} \quad (2.3)$$

where, the lower subscripts of u, v, and T in terms of x and y denote the partial derivatives of respective order.

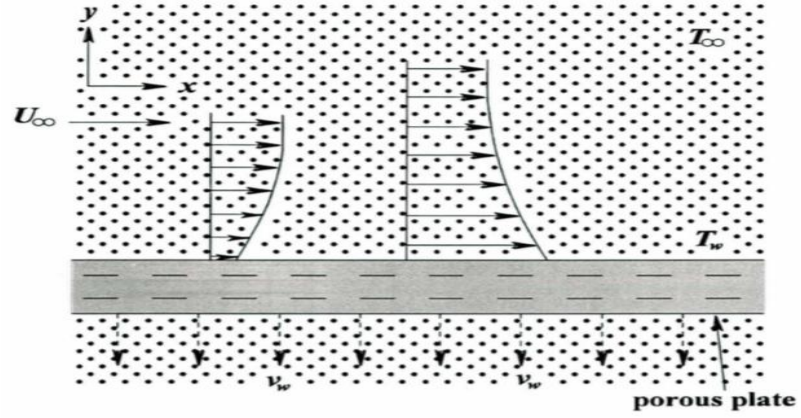

Figure 1: Fluid model depicting geometry of the flow

The relevant boundary conditions taking slip effects are as follows:

$u = G_1 u_y\,, v = v_w$ at y = 0; $u \to U_\infty$ as $y \to \infty$ (2.4)

T=T_W+H_1 T_y at y=0 ; →T_∞ as →∞ (2.5)

W here, $G_1 = G_0(Re_x)^{\frac{1}{2}}$, $H_1 = H_0(Re_x)^{\frac{1}{2}}$, $Re_x = \frac{U_\infty x}{\nu} v_w = \frac{v_0}{(x)^{\frac{1}{2}}}$.

A careful inspection gives the following set of similarity transformations:

$\Psi = \sqrt{U_\infty \nu x}\, f(\eta), T = T_\infty + (T_w - T_\infty)\theta(\eta)$, and$\eta = \frac{y}{x}\sqrt{Re_x}$, (2.6)

W here Ψ: stream function satisfying $u = \frac{\partial \Psi}{\partial y}$and $v = -\frac{\partial \Psi}{\partial x}$, θ: temperature function andη: similarity variable.

Using similarity transformations, equations (2.6), (2.2) and (2.3) finally reduced to self-similar forms as follows:

$$f''' + \frac{1}{2} f f'' + k_1[2f' f''' + f f'^{\mathrm{v}} - (f'')^2] + k^*(1 - f') = 0 \quad (2.7)$$

$$\theta'' + \frac{1}{2} Pr f \theta' = 0 \quad (2.8)$$

W here $k_1 = \frac{k_0 U_\infty}{2\mu x}$, $k^* = \frac{1}{Da_x Re_x}$, $Da_x = \frac{k}{x^2}$,,$Pr = \frac{\mu C_p}{K}$.

The reduced form of boundary conditions (2.5) and (2.6) are:

$At\ \eta = 0, f(\eta) = S,\ f'(\eta) = \delta f''(\eta);\ as\ \eta \to \infty,\ \ f'(\eta) = 1,\ f''(\eta) = 0$ (2.9)

$At\ \eta = 0, \theta(\eta) = 1 + \beta\theta'(\eta);\ as\ \eta \to \infty, \theta(\eta) = 0$ (2.10)

W here, $S = \left(-\frac{2v_w}{U_\infty}\right)(Re_x)^{\frac{1}{2}} = -\frac{2,v_0}{(U_\infty \nu)^{\frac{1}{2}}}$, $\delta = \frac{G_0 U_\infty}{\nu}$, $\beta = \frac{H_0 U_\infty}{\nu}$.

2. **Method of Solution:** To utilize the 'bvp4c' solver of MATLAB [16, 17], the governing equations (2.7) and (2.8) along with the boundary conditions (2.9) and (2.10) can be expressed in a reduced form as:

$$f_4' = \frac{1}{f_1}\left[(f_3)^2 - 2f_2 f_4 - \left(\frac{1}{k_1}\right)\left\{f_4 + \frac{1}{2}f_1 f_3 + k^*(1 - f_2)\right\}\right] \quad (3.1)$$

$$f_6' = -\frac{1}{2}Pr f_1 f_6 \quad (3.2)$$

$$f_1(0) = S, f_2(0) = \delta f_3(0)\ and\ f_2(\infty) = 1, f_3(\infty) = 0 \quad (3.3)$$

$$f_5(0) = 1 + \beta f_6(0)\ and\ f_5(\infty) = 0 \quad (3.4)$$

Considering $f_1 = f, f_2 = f', f_3 = f'', f_4 = f''', f_5 = \theta, f_6 = \theta'$

The 'bvp4c' solver, which is a built-in function in MATLAB, is utilized to calculate the aforementioned equations along with various flow feature parameters involved.

3. **Results and Discussion:** The expressions for velocity $(\boldsymbol{f'(\eta)})$, temperature $(\boldsymbol{\theta(\eta)})$, temperature gradient at the plate ($-\boldsymbol{\theta'(0)}$) and skin friction coefficient ($\boldsymbol{\tau}$) are obtained numerically employing MATLAB 'bvp4c' solver for involved dimensionless flow feature parametersi.e., viscoelastic parameter ($\mathbf{k_1}$), permeability parameter ($\mathbf{k}^*$), Prandtl parameter ($\boldsymbol{Pr}$), velocity slip parameter (δ), thermal slip parameter ($\boldsymbol{\beta}$), suction/blowing parameter ($\mathbf{S}$). The computed results are depicted graphically to observe the impact of involved flow parameters on Newtonian fluid and viscoelastic non-Newtonian fluid respectively for comparison purpose. The results of Newtonian fluid are obtained easily by setting $\mathbf{k_1 = 0}$.

To evaluate the accuracy of the numerical results evaluatedby 'bvp4c' solver and to validate the current study, the skin friction is calculated without taking viscoelastic and permeability factors and is obtained as $\boldsymbol{f''(0) = 0.3321}$ which is well in accord with the standard results obtained by Howarth [3] as $\boldsymbol{f''(0) = 0.33206}$ and Bhattacharyya and Layek [9] as $\boldsymbol{f''(0) = 0.332058}$.

Figs. 2- 4.3 illustrate the velocity distribution for variation of permeability, suction and velocity slip flow parameters on the Newtonian fluid and viscoelastic non-Newtonian fluid. The velocity curve $\boldsymbol{f'(\eta)}$ tends to 1 very rapidly as $\boldsymbol{\eta}$ →2.5 and thus considering 2.5 as infinity appears to justify the boundary conditions at infinity. Fig. 2 (a) shows that the velocity over the plate enhances as the permeability parameter increases because the Darcian body force reduces as the permeability parameter increases, leading to a reduction in the drag experienced by the flow, which helps to improve fluid motion.

However, as shown in Fig. 2 (b), the velocity $\boldsymbol{f'(\eta)}$on the plate decelerates as the value of k rises. As the fluid is viscoelastic, so considerable high drag is accomplished and thus the velocity is retarded.

Figs. 3 (a) and 3 (b) display the velocity curves for suction parameters S. The fluid motion accelerates as the suction parameter rises, as shown in Fig. 3 (a).The process of sucking fluid particles through a porous wall slows the creation of the fluid boundary layer. Suction has the effect of drawing fluid close to the wall, thereby decreasing the momentum boundary layer and enhancing fluid velocity. But it is noticed from 3 (b) that the flow rate decelerates with increasing values of S.As fluid particles are absorbed into the porous plate, the fluid motion decreases, resulting in a thinner velocity boundary layer.

Figures 4 (a) and 4 (b) illustrate the velocity profile $\boldsymbol{f'(\eta)}$for different values of slip factor δ.As the slip factor δ rises due to frictional resistance between the fluid and the boundary surface, the rate of fluid transport accelerates in both Newtonian fluid and viscoelastic non-Newtonian fluid. Because of the slip, positive values of velocity near the plate are seen, and the thickness of the momentum boundary layer is reduced. The thermal slip parameter $\boldsymbol{\beta}$ has no effect on the velocity profiles since the momentum equation is independent of $\boldsymbol{\theta}$.

The temperature curves are graphically presented in Figs. 5-8 for different values of permeability, suction, velocity, and thermal slip flow parameters. The fluid temperature diminishes with the growth of permeability factor, as shown in Fig. 5 (a). The thickness of the thermal boundary layer is reduced as the permeability factor k* is increased. It is noticed from 5 (b) that the fluid temperature accelerates with the rise of permeability factor and thus we can conclude that thethermal boundary layer thickness enhances with the rising permeability. Growing permeability helps to improve fluid temperature by reducing the thickness of the momentum boundary layer.

The temperature distribution for different values of S is depicted in Figs.6 (a) and 6 (b). It is observed that the fluid temperature diminishes with the rise of the suction factor. Heat transport increases when the thickness of the thermal boundary layer decreases. As the suction values increase, the fluid is drawn closer to the plate, resulting in a decrease in fluid temperature. Figs.7 (a) and 7 (b) indicate that the fluid temperature diminishes as slip factor δ enhances for both Newtonian and viscoelastic fluids and thus less heat is deported from the flat permeable plate to the fluid domain. A high rate of fluid motion is observed near the plate due to the slip factor which enhances the heat transfer. The effect of the thermal slip factor $\boldsymbol{\beta}$ on the temperature profile for Newtonian and visco-elastic fluids is shown in Figs.8 (a) and 8 (b). The temperature drops as the thermal slip factor increases because less heat is transported from the permeable flat plate to the fluid domain.

The heat transport rate from the plate, which is represented by the temperature gradient $\boldsymbol{-\theta'(0)}$ are plotted against the velocity and thermal slip factors δ and $\boldsymbol{\beta}$ respectively in Figs. 9-10 for Newtonian fluid and viscoelastic non-Newtonian fluid for variation of permeability factor k*.Fig. 9 (a) illustrates the heat transport rate and it shows

that it enhances with the growth of both velocity slip and permeability parameters. Fig. 9 (b) indicates that for non-Newtonian fluids, the heat transport rises as the velocity slip parameter is enhanced, but diminishes when the permeability parameter increases. The heat transport rate at the plate rises with the growth of the thermal slip factor but diminishes for growing permeability for Newtonian fluid, as observed in Fig. 10 (a) but for viscoelastic non-Newtonian fluid, the heat transport rate at the plate reduces for rising values of thermal slip and permeability parameters, as noticed in Fig. 10 (b).

The coefficient of skin friction is a significant physical parameter that quantifies the resistance caused by viscosity on the plate surface. Figures 11 (a) and 11 (b) illustrate the relationship between the skin friction coefficient 'τ' and the slip factor 'δ' for distinct values of permeability factor k* for both Newtonian and viscoelastic fluids. The viscous drag diminishes gradually with the rise of slip factor but it enhances with the growth of permeability factor as noticed in Fig. 11 (a). From Fig.11 (b), it is noticed that the friction at the plate reduces rapidly with the growth of permeability and thus more fluid passes through the plate and approaches to zero as slip parameters are enhanced.

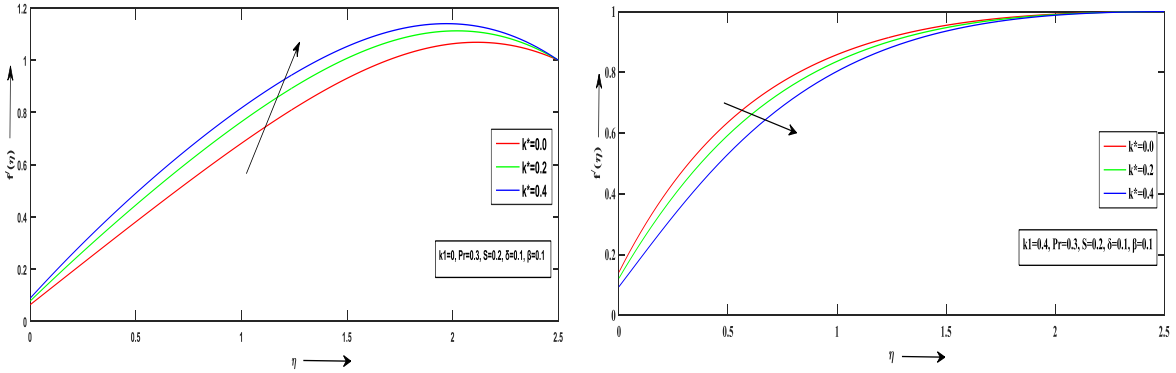

(a) Newtonian fluid **(b)** Viscoelasticfluid

Figure 2: Effects of k * on velocity curve $f'(\eta)$ against η

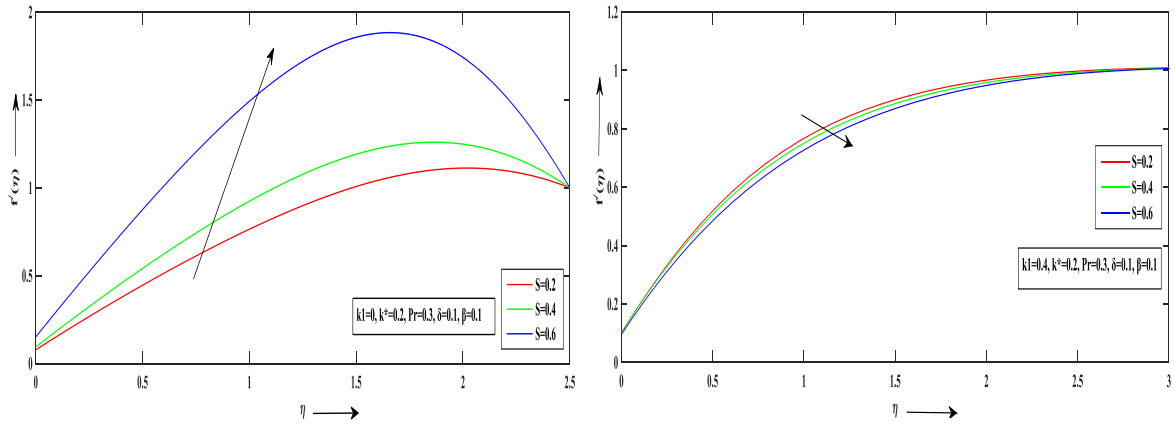

(a) Newtonian fluid **(b)** Viscoelastic fluid

Figure 3: Effects of S on velocity curve $f'(\eta)$ against η

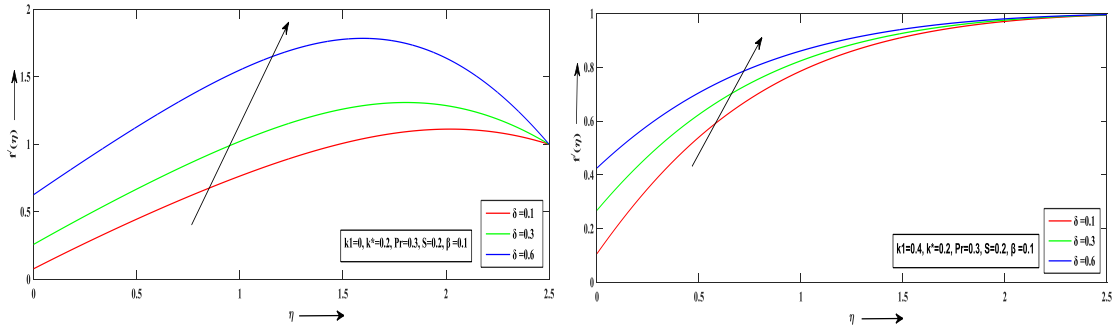

(a) Newtonian fluid **(b)** Viscoelastic fluid

Figure 4: Effects of δ on velocity curve $f^{'}(\eta)$ against η

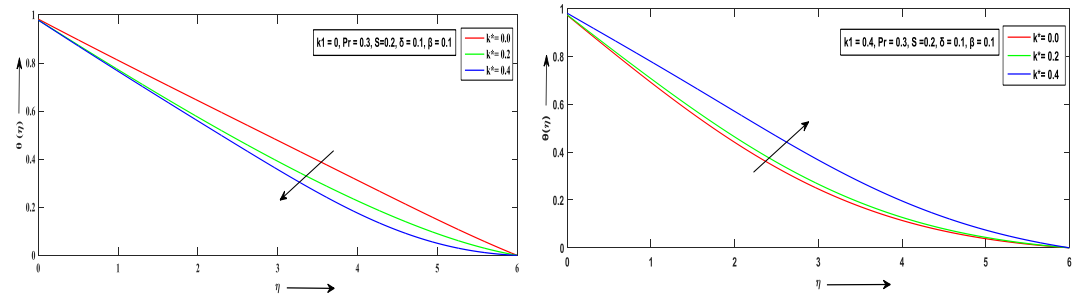

(a) Newtonian fluid **(b)** Viscoelastic fluid

Figure 5: Effects of k* on temperature curve $\theta(\eta)$ against η

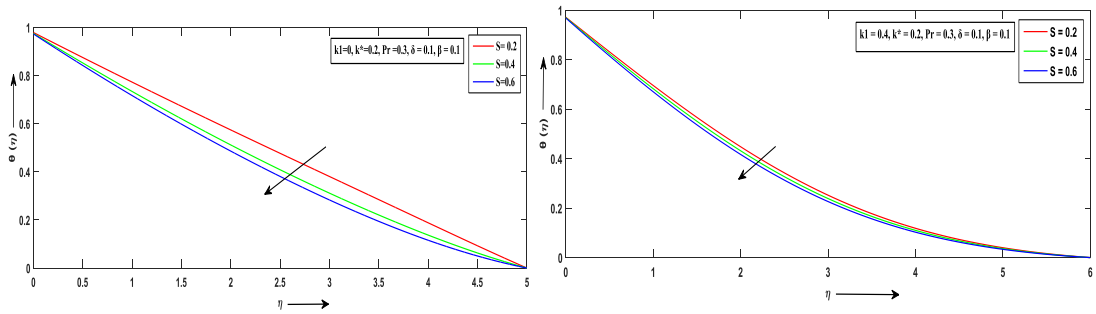

(a) Newtonian fluid **(b)** Viscoelastic fluid

Figure 6: Effects of S on temperature curve $\theta(\eta)$ against η

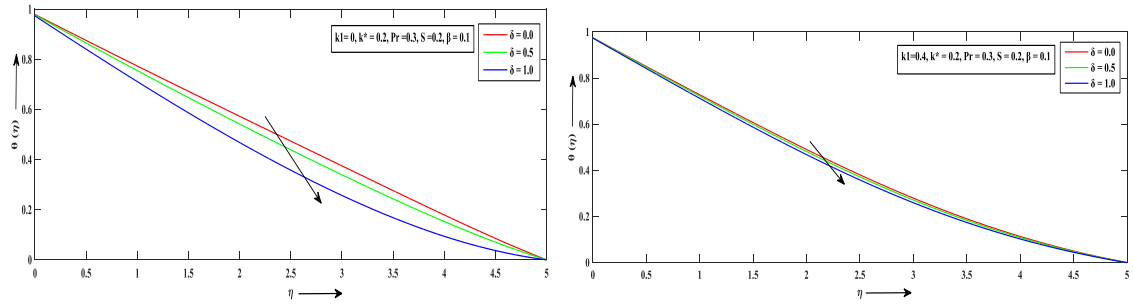

(a) Newtonian fluid **(b)** Viscoelastic fluid

Figure 7: Effects of δ on temperature curve $\theta(\eta)$ against η

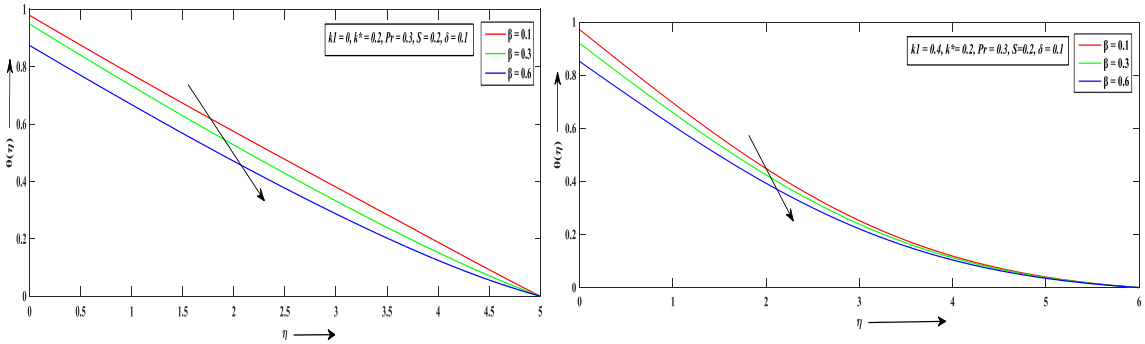

(a) Newtonian fluid **(b)** Viscoelastic fluid

Figure 8: Effects of β on temperature curve $\theta(\eta)$ against η

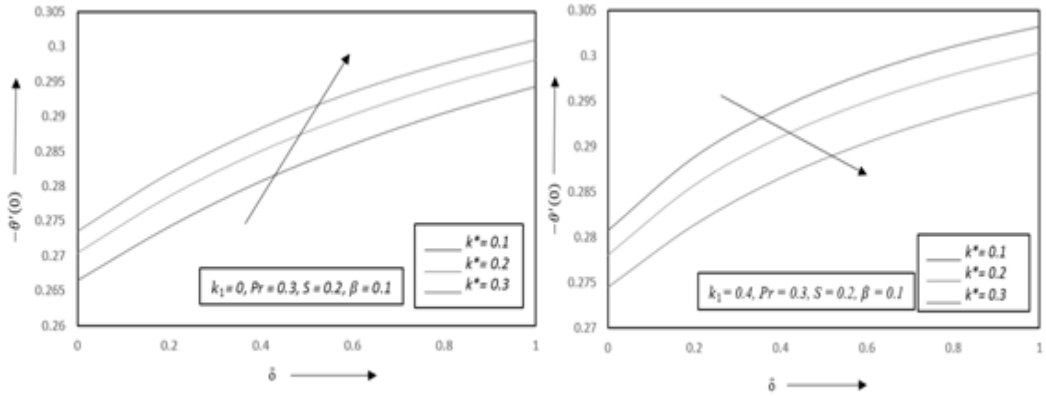

(a) Newtonian fluid **(b)** Viscoelastic fluid

Figure 9: Effects of k* on temperature gradient curve $-\theta'(0)$ against δ

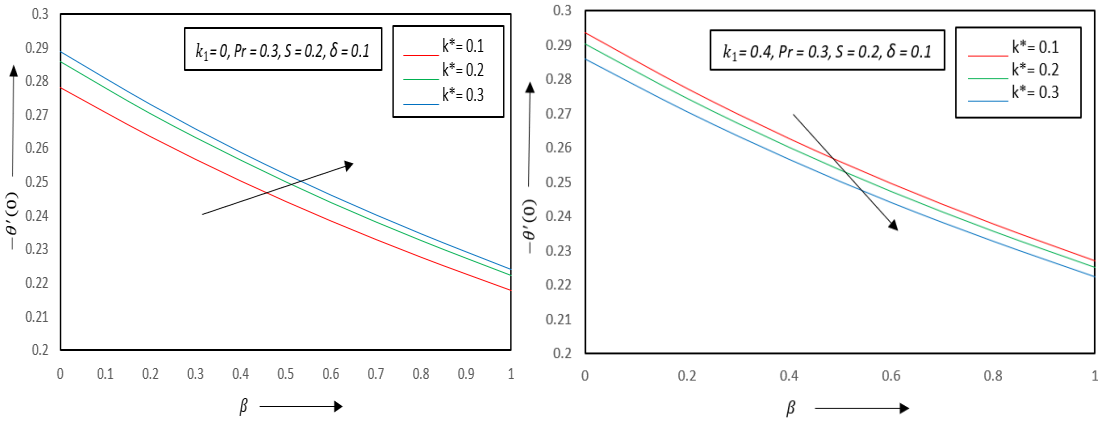

(a) Newtonian fluid **(b)** Viscoelastic fluid

Figure 10: Effects of k* on temperature gradient curve $-\theta'(0)$ against β

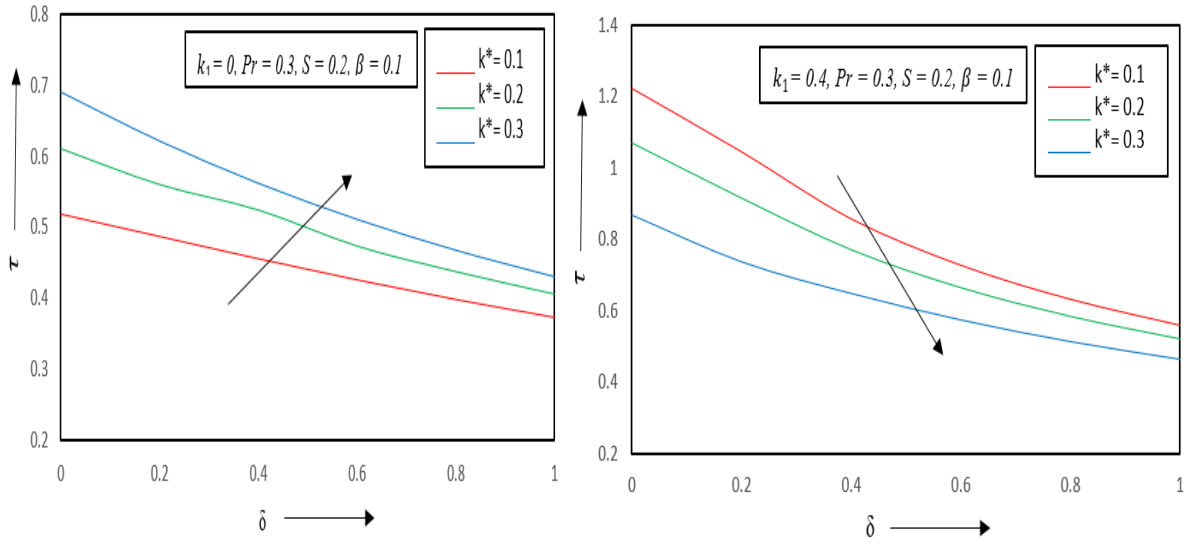

(a) Newtonian fluid **(b)** Viscoelastic fluid

Figure 11: Effects of k* on skin friction coefficient τ against δ

II. CONCLUSION

This work has significant potential for further research due to its potential use in several subfields of engineering science. Some fluid properties have been discussed in this study, but there are many rheological properties of fluids of engineering interest that may be incorporated for further research. In light of the information presented in this paper, we can conclude that:

- The growth of permeability and suction parameter enhances the fluid motion for Newtonian fluid, but the reverse pattern of flow is observed for viscoelastic non-Newtonian fluid.
- The rate of fluid transport is enhancedfor Newtonian as well as viscoelasticfluids as the slip factor δ rises.
- The fluid temperature decreases with the growing permeability parameter for Newtonian fluid, but for non-Newtonian fluid growing permeabilityhelps to enhance the fluid temperature.
- The rising values of suction and slip parameters diminish the heat transport in both Newtonian and viscoelastic fluids.
- The heat transport rate enhances with growing permeability for Newtonian fluid but for viscoelastic fluid, it diminishes in presence of slip factors.
- The viscous drag diminishes gradually with the rise of the slip factor, but it enhances with the growth of the permeability factor for Newtonian fluid but,in case of viscoelastic fluid, it diminishes with the growth of slip and permeability parameters.

III. NOMENCLATURE

u	fluid motion along x-axis
v	fluid motion along y-axis
ν	kinematic viscosity
k	permeability parameter
k_0	viscoelastic parameter
ρ	fluid density
U_∞	free stream velocity
T	temperature
C_p	specific heat
K	thermal conductivity
G_1	velocity slip factor
G_0	initial velocity slip flow factor
H_1	thermal slip factor
H_0	initial thermal flow slip factor
T_W	constant plate temperature
T_∞	free stream temperature
Re_x	local Reynolds number
v_w	suction or blowing parameter
k_1	modified viscoelastic parameter
k^*	modified permeability parameter
Da_x	local darcy number
Pr	prandtl number
S	Modified suction or blowing
δ	modified velocity slip factor
β	modified thermal slip factor”

REFERENCES

[1] Blasius, H. (1908). Greenzschichten in FliissigkeitenmitkleinerReibung. *Z. Math. U. Phys.*, 56, 1-37.
[2] Pohlhausen, E. (1921). OerWarmeaustauschzwischenfestenKorpem und FliissigkeitenmitkleinerReibung und kleinerWarmeleitung. *Z. Angew. Math. Mech*., 1, 151-121.
[3] Howarth, L. (1939). On the solution of the laminar boundary layer equations. *Proc. Roy. Soc. London A*., 164, 547-579.

[4] Cheng, P., Minkowycz, W.J. (1977). Free convection about a vertical flat plate embedded in a porous medium with application to heat transfer from a disk. *J. Geophys. Res*., 88, 2040-2044.
[5] Rabadi, N.J., Hamdan, E.M. (2000). Free convection from inclined permeable walls embedded in variable permeability porous media with lateral mass flux. *J. Petrol. Sci. Eng*., 26, 241-251.
[6] Mukhopadhyay, S., Layek, G.C. (2009). Radiation effect on forced convective flow and heat transfer over a porous plate in a porous medium. *Meccanica*, 44, 587-597.
[7] Ishak, A. (2010). Similarity solutions for flow and heat transfer over a permeable surface with convective boundary conditions. *Appl. Math. Comput*., 217, 837-846.
[8] Bhattacharyya, K., Layek, G.C., Reddy, R.S. (2012). Slip Effect on Boundary Layer Flow on a Moving Flat Plate in a Parallel Free Stream. *International Journal of Fluid Mechanics Research*, 39, 438-447.
[9] Bhattacharyya, K., Layek, G.C. (2012). Similarity solution of MHD boundary layer flow with diffusion and chemical reaction over a porous flat plate with suction/blowing. Meccanica, 47, 1043-1048. DOI 10.1007/s11012-011-9461-x.
[10] Abbas, Z., Wang, Y., Hayat, T., Oberlack, M. (2009). Slip effects and heat transfer analysis in a viscous fluid over an oscillatory stretching surface. *Int. J. Numer. Method H.*, 59, 443-458.
[11] Khan, W.A., Khan, Z.H., Rahi, M. (2014). Fluid flow and heat transfer of carbon nanotubes along a flat plate with navier slip boundary. *Applied Nanoscience*, 4, 633-641.
[12] Ambreen, A.K., Hafsa, U., Vafai, K., R Ellahi, R. (2016). Study of peristaltic flow of magnetohydrodynamics Walter's B fluid with slip and heat transfer. *Int. J, Sci. Tech*., 23, 2650-2662.
[13] Sarojamma, G., Sreelakshmi, K., Vajravelu, K. (2018). Effects of dual stratification on non-orthogonal Non-Newtonian fluid flow and heat transfer. International journal of Heat and Technology, 36(1), 207-214. https://doi.org/10.18280/ijht.360.
[14] Walters, K., (1960), The motion of an elastico-viscous liquid contained between co-axial cylinders. Q. J. Mech. Appl. Math.,13, 444-456.
[15] Walters, K., (1962), The solutions of flow problems in the case of materials with memories, J. Mecanique 1, 473-478.
[16] Ascher, U., Mattheij, R., & Russell, R. (1995). Numerical solution of boundary value problems for ordinary differential equations. SIAM, Philadelphia, PA.
[17] Kierzenka, J. and Shampine, L.F. (2001). A BVP Solver Based on Residual Control and the MATLAB PSE. ACM Transaction on Mathematical Software, 27(3), 299-316. http://doi.org/10.1145/502800.502801

